



**HAL**  
open science

## **Behaviour of individual VOCs in indoor environments: How ventilation affects emission from materials**

Florent Caron, Romain Guichard, Laurence Robert, Marie Verrièle, Frederic Thevenet

### ► **To cite this version:**

Florent Caron, Romain Guichard, Laurence Robert, Marie Verrièle, Frederic Thevenet. Behaviour of individual VOCs in indoor environments: How ventilation affects emission from materials. Atmospheric Environment, 2020, 243, pp.117713. 10.1016/j.atmosenv.2020.117713 . hal-03040782

**HAL Id: hal-03040782**

**<https://hal.science/hal-03040782v1>**

Submitted on 5 Sep 2022

**HAL** is a multi-disciplinary open access archive for the deposit and dissemination of scientific research documents, whether they are published or not. The documents may come from teaching and research institutions in France or abroad, or from public or private research centers.

L'archive ouverte pluridisciplinaire **HAL**, est destinée au dépôt et à la diffusion de documents scientifiques de niveau recherche, publiés ou non, émanant des établissements d'enseignement et de recherche français ou étrangers, des laboratoires publics ou privés.



Distributed under a Creative Commons Attribution - NonCommercial 4.0 International License

# 1            **Behaviour of individual VOCs in indoor environments: how** 2            **ventilation affects emission from materials**

3 Florent Caron<sup>1,2\*</sup>, Romain Guichard<sup>1</sup>, Laurence Robert<sup>1</sup>, Marie Verrièle<sup>2</sup>, Frédéric  
4 Thevenet<sup>2</sup>

5 <sup>1</sup>French institute of research and safety (INRS), Department of Process Engineering, Rue du Morvan,  
6 54519 Vandoeuvre-lès-Nancy, France

7 <sup>2</sup>IMT Lille Douai, University of Lille, SAGE department, 59000 Lille, France

8 \*Corresponding author. E-mail address: florent.caron@inrs.fr

## 9    **Abstract**

10 Indoor air quality is affected by both emissions of Volatile Organic Compounds (VOC) from  
11 materials and ventilation. The purpose of this paper is to provide a multi-scale analysis of the  
12 impact of ventilation on VOC emissions to highlight the individual behaviours of VOCs  
13 emitted from a wood particleboard. Emissions were studied in an experimental chamber by  
14 (i) assessing the effect of ventilation on emission rates and (ii) determining intrinsic  
15 parameters ( $K_i$ ,  $C_{0,i}$ ,  $D_i$ ) describing the VOC mass transfer from the material to air. The  
16 overall assessment of the effect of ventilation indicated that the air change rate could  
17 significantly affect the behaviour of individual compounds. Typically, the formaldehyde  
18 emission rate increased from 214.6 to 274.2  $\mu\text{g}\cdot\text{m}^{-2}\cdot\text{h}^{-1}$  when air change rate varies from 2.5  
19 to 5.5  $\text{h}^{-1}$ , whereas the air speed had no influence on emission rates for any VOC monitored.  
20 These results agree with the key emission parameters (partitioning and diffusion coefficients)  
21 which were higher for formaldehyde than those for other compounds. VOC diffusion related  
22 to VOC mass transfer from a material's surface to the surrounding air was the limiting step in  
23 VOC emission for the solid material studied, and should therefore be considered when  
24 developing ventilation strategies.

## 25    **Keywords**

26 ventilation ; formaldehyde ; VOC ; partitioning coefficient ; diffusion coefficient ; initial  
27 emittable concentration

## 28 **1. Introduction**

29 Modern lifestyles and climate mean that people spend more than 80% of their time in indoor  
30 environments such as public transport, the home or workplace (Zhang et al., 2012). In these  
31 environments, internal sources of emissions are the major contributors to poor air quality.  
32 Among the large variety of indoor pollutants, Volatile Organic Compounds (VOCs) are the  
33 most studied, because of their ubiquity and their indisputable negative impacts on human  
34 health (Wolkoff and Nielsen, 2001). Although the indoor concentrations of VOCs are low – in  
35 the ppb range – the exposure profile tends to be chronic. Long-term exposure to VOCs can  
36 lead to skin irritation, dizziness, and tiredness, as well as damage to pulmonary function  
37 (Yoon et al., 2010).

38 Among known prevention strategies, ventilation is usually recommended to reduce indoor  
39 VOC concentration. Indeed, these concentrations are simultaneously governed by both the  
40 sources of emission and the level of ventilation. Air change allows extraction and dilution to  
41 reduce the VOC concentrations from indoor sources (de Gennaro et al., 2014). However, if  
42 the ventilation is insufficient to balance indoor emissions, or if the incoming air is itself  
43 polluted, VOC concentrations tend to increase (Shang et al., 2016). To address the  
44 connection between ventilation and indoor air quality in stores, field measurement campaigns  
45 were carried out in a sports store under forced and natural ventilation conditions (Robert et  
46 al., 2018). Results indicated that, unlike other VOCs monitored, formaldehyde concentrations  
47 are not directly indexed on the ventilation condition. This result was supported by other  
48 studies, with Hun et al. (2010), Offermann and Hodgson, (2011) and Nirlo et al. (2014)  
49 reporting for equivalent real case studies showing a lack of correspondence between the  
50 concentration of formaldehyde and the air change rate (ACR). According to these references,  
51 a high ACR tends to promote VOC emissions, especially for formaldehyde, which may  
52 present a different behaviour compared to other VOCs.

53 Contradictory trends can also be found in the literature: in their on-site studies, Hult et al.  
54 (2015) and Huang et al. (2017) report that the formaldehyde concentration negatively

55 correlates with the ventilation rate. In addition, some laboratory experiments conducted  
56 under controlled conditions show that the ventilation significantly affects VOC emission rates  
57 (Knudsen et al., 1999; Myers, 1982), with the air speed over the material's surface having a  
58 marked impact (Hun et al., 2010; Knudsen et al., 1999). According to Hult et al. (2015), this  
59 effect of ventilation is related to a combination of (i) the ACR and (ii) the air velocity close to  
60 the material's surface. The influence of ventilation on the resulting VOC concentrations or  
61 directly on the VOC emission rate has not been clearly established. Given their contrasting  
62 behaviour, VOCs should be individually considered when investigating emissions from solid  
63 materials.

64 In addition, the mass transfers of VOCs are governed by elementary and mostly reversible  
65 mechanisms including convective mass transfer through the boundary layer, VOC diffusion  
66 within the solid material and, VOC sorption on the material's surface, which is characterized  
67 by an equilibrium between the solid material phase and the carrier gas phase (Tiffonnet et  
68 al., 2006). Consequently, VOC emissions from a solid material are controlled by a  
69 combination of diffusion within the material and mass transfer across the boundary layer in  
70 various extents (Wolkoff, 1998).

71 According to the literature, VOC emissions from a solid material can be described by three  
72 key emission parameters for a VOC  $i$ , at fixed temperature and relative humidity (RH) (Cox et  
73 al., 2010; Liu et al., 2013):

74 (i) The partitioning coefficient  $K_i$  reflects the ability of VOC  $i$  to transfer from the adsorbed  
75 phase to the gas phase according to a reversible equilibrium relationship between  
76 the material and the air

77 (ii) The initial emittable concentration  $C_{0,i}$  ( $\text{mg}\cdot\text{m}^{-3}$ ) corresponds to the initial concentration  
78 of VOC  $i$  within the material that is available for emission into the surrounding air

79 (iii) The diffusion coefficient within the solid material  $D_i$  ( $\text{m}^2.\text{s}^{-1}$ ) is described by the Fick's  
80 second law, considering a constant one-dimensional diffusion of VOC  $i$  in a  
81 homogeneous material

82 In specific ventilation conditions, the convective mass transfer coefficient  $h_i$  for VOC  $i$  may  
83 also be needed to describe mass transfer through the boundary layer. This parameter can be  
84 determined using the theoretical equation proposed by Axley (1991).

85  $K_i$ ,  $C_{0,i}$  and  $D_i$  can be experimentally determined by adapting protocols from the literature,  
86 generally under constant temperature and RH conditions. Most published experimental  
87 protocols address each parameter independently. For example, the multi-flushing extraction  
88 method can be used to determine  $C_{0,i}$  (Smith et al., 2009), whereas the porosity test method  
89 determines  $D_i$  (Xiong et al., 2008). Some experimental methods allow the two parameters to  
90 be simultaneously determined, such as the two-chamber method (Bodalal et al., 2000) and  
91 the micro-balance method (Liu et al., 2014). However, these approaches must be combined  
92 with other protocols to access the three key emission parameters. Only two methods to  
93 simultaneously determine the three parameters in a single experiment have been reported in  
94 the literature to date: (i) the C-history method (S. Huang et al., 2013) and (ii) the alternately  
95 airtight/ventilated emission method proposed by Zhou et al. (2018).

96 Based on the study by Tiffonnet (2000), two complementary approaches for studying VOC  
97 emission phenomena can be considered:

98 (i) The *chamber scale approach* monitors VOC concentration profiles emitted from a  
99 solid material placed in an experimental chamber under controlled experimental  
100 conditions. Based on the recorded profile, VOC emission rates can be calculated  
101 from the mass balance and the experimental conditions when the steady state is  
102 reached. This approach provides an overall characterization of the VOC emission  
103 process at macroscopic scale.

104 (ii) The *material scale approach* is based on the laws governing the mass transfer  
105 phenomenon and reflects the elementary mechanisms involved in the holistic  
106 interaction processes between a solid material and the air. The resulting VOC  
107 concentrations are expressed as a function of the physical parameters describing  
108 the state of the systems studied. Some of these parameters characterize the  
109 intrinsic properties of the material involved in the emission processes.

110 The main purpose of this paper is to address individual VOC behaviour based on a detailed  
111 analysis of the impact of ventilation on emissions of target VOCs from a typical material. The  
112 chamber scale approach was used with a reduced-scale experimental chamber to study total  
113 VOC emissions. Then, the material scale approach was used to determine the inherent  
114 characteristics of the material that directly govern VOC transfers from the material to the  
115 surrounding air. Finally, the contribution of each approach was assessed, and their  
116 interactions were determined to improve our understanding of VOC emission phenomena.

## 117 **2. Materials and methods**

### 118 **2.1. Experimental strategy**

#### 119 **2.1.1. Chamber scale approach**

120 Although the impact of ventilation on VOC emissions has been widely investigated in  
121 laboratory experiments, Knudsen's group are one of the few to have highlighted an impact of  
122 air speed on VOC emissions from a solid material (Knudsen et al., 1999). However, the  
123 respective roles of the ACR and air velocity are not clearly discriminated in most  
124 experimental studies (Risholm-Sundman, 1999; Uhde et al., 1998; Wolkoff, 1998). The  
125 chamber scale approach consists in experimentally studying VOC emissions from a solid  
126 material using a ventilated experimental chamber, which allows independent control of the  
127 ACR and the air velocity over the material's surface. The resulting concentrations and  
128 emission rates for the main VOCs, including formaldehyde, can thus be determined under  
129 non-identical ventilation regimes. By discriminating between the ACR and the air velocity, it  
130 was possible to highlight and assess their respective effect on VOC emission processes.

### 131 **2.1.2. Material scale approach**

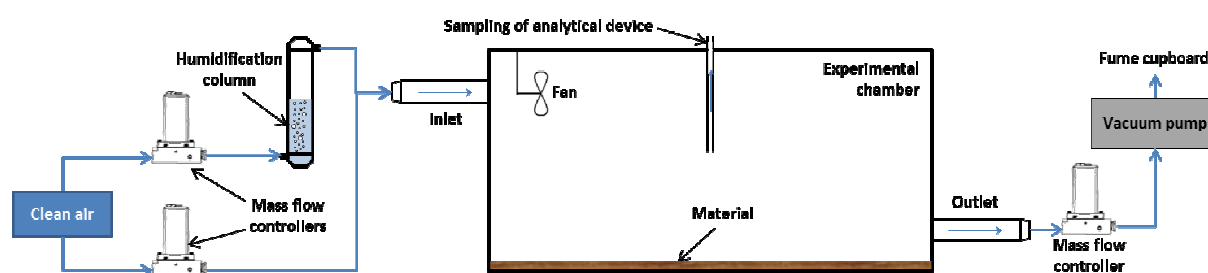
132 The two experimental protocols simultaneously determining the three key emission  
133 parameters provide equivalent accuracy and efficiency (S. Huang et al., 2013; Zhou et al.,  
134 2018). Although experiments can be carried out over reasonable time scales, the C-history  
135 method (S. Huang et al., 2013) involves many intermediate parameters and complex data  
136 processing. Consequently, fluctuating experimental data may generate extensive deviations  
137 in the results. The method proposed by Zhou et al. (2018) was therefore preferred since it  
138 involves less data processing, despite requiring more experimental abilities than the C-  
139 history method. The material scale approach used here consisted in determining the three  
140 key emission parameters for the main VOCs emitted by a solid material. The emission  
141 parameters are determined by adapting the experimental protocol developed by Zhou et al.  
142 (2018) to the experimental ventilated chamber used.

## 143 **2.2. Experimental setup**

### 144 **2.2.1. Ventilated chamber**

145 All experiments were carried out in a 128-L aluminium ventilated experimental chamber with  
146 inner dimensions of 0.8x0.4x0.4 m (Figure 1). The inlet and outlet ports of the chamber  
147 present circular sections with a diameter of 0.04 m, and are located on opposite faces of the  
148 chamber. The main axes of the inlet and outlet ports are located in the centre of each face, at  
149 0.055 m from the top and 0.055 m from the bottom of the experimental chamber respectively.  
150 Flow of fresh air introduced into the chamber was controlled by BROOKS mass flow  
151 controllers, with an operation range of 0-20 L.min<sup>-1</sup> ± 0.25%. The fresh air from the generator  
152 contained residual impurity levels below the resolution of the analytical device. The mass  
153 balance between the inlet and the outlet was ensured by a system composed of a mass flow  
154 controller and a vacuum pump to maintain a constant outlet flow equal to the inlet flow. Given  
155 this equilibrium between the inlet and the outlet airflow, the difference of pressure between  
156 the open atmosphere and the chamber was negligible.

157 The air temperature in the chamber was controlled by the laboratory's temperature. This  
158 temperature is regulated by an air conditioning system set to  $21 \pm 0.5$  °C. RH in the chamber  
159 was controlled by passing the incoming airflow through a column filled with water. The ratios  
160 of dry and water-saturated airflow rates introduced into the chamber could be adjusted to  
161 attain the desired RH. All experiments were performed at a RH of  $50 \pm 5$  %. Temperature  
162 and RH conditions were continuously monitored using respectively a Pt 100 sensor with  
163 resolution of 0.1 °C and a capacitive sensor with resolution of 0.1 %RH from a KIMO probe  
164 placed inside the chamber.



165

166 **Figure 1. Experimental setup showing the 128 L aluminium ventilated chamber.**

167 A mixing fan was placed close to the ceiling of the chamber and oriented in the direction of  
168 the main axis of the inlet flow at 0.1 m from the inlet port. This fan, measuring 127x127x38  
169 mm, generated an airflow of  $270 \text{ m}^3 \cdot \text{h}^{-1}$  at a nominal voltage of 12 V. The ACR was controlled  
170 by mass flow controllers, whereas the mixing fan regulated mixing of the air inside the  
171 experimental chamber.

### 172 **2.2.2. Selected material**

173 The sample used for this paper was a commercial wood particleboard (PB) with a waterproof  
174 coating, considered a model material. This material was chosen for its simple geometry, the  
175 diversity of VOCs it emits, and its wide use in indoor environments as well as because many  
176 studies have examined VOC emissions from construction materials. The 0.015-m-thick wood  
177 panel measuring 0.795x0.395 m was placed inside the experimental chamber with only one  
178 face of the panel exposed. PBs from the same batch were used for each series of tests. All

179 panels were packaged in plastic film and stored in a light-protected area in the air-  
180 conditioned laboratory to avoid any VOC depletion as a result of passive emissions into the  
181 air.

### 182 **2.2.3. VOC monitoring**

183 The diversity of C6 – C16 VOCs and carbonyl compounds emitted from the PB in the air  
184 chamber was initially screened using off-line measurement methods. To do so, air samples  
185 were collected from the chamber onto DNPH and TENAX sorbent cartridges. DNPH  
186 cartridges were desorbed with acetonitrile and analysed using an UltraViolet – High  
187 Performance Liquid Chromatography (UV-HPLC) system. TENAX sorbent cartridges were  
188 thermally desorbed and analysed using a Thermal Desorption-Gas Chromatograph equipped  
189 with Flame Ionization and Mass Spectrometer detectors (TD/GC-FID-MS). Chromatographic  
190 analyses revealed that the main VOCs emitted from the PB were: acetone, acetaldehyde,  
191 formaldehyde, propanal, butanal, pentanal, hexane and mono-terpenoid compounds  
192 including  $\alpha$ -pinene,  $\beta$ -pinene, limonene, 3-carene, camphene, and  $\alpha$ -phellandrene. These  
193 VOCs were therefore specifically monitored in subsequent experiments.

194 Throughout the emission vs. ventilation experiments, VOCs were monitored using an online  
195 Selected Ion Flow Tube – Mass Spectrometer (SIFT-MS). This instrument relies on the  
196 positive chemical ionization technique, but does not require specific sample preparation or  
197 pre-concentration. First, ions are formed by microwave discharge on wet air at low pressure.  
198 A first quadrupole alternatively selects  $\text{H}_3\text{O}^+$ ,  $\text{NO}^+$  and  $\text{O}_2^+$  ions. Selected ions and analytes  
199 then enter the flow tube, where specific product ions are formed and separated according to  
200 their mass-to-charge ratio ( $m/z$ ). These products are detected using a second quadrupole.  
201 Concentrations were calculated after calibration based on the signal intensity of each VOC  
202 with a resolution of 1 ppb. The limits of detection (LoD) of our analytical procedure were  
203 calculated from blank measurements, and are reported in Table 1. The reagent ions and  
204 product ions monitored for this study are listed in Table 1 for each VOC monitored. Since the  
205 principle of the mass spectrometry detector is to separate compounds according to their

206 mass, the mass resolution of the SIFT-MS device cannot discriminate between the different  
 207 mono-terpenes emitted from the wood PB. “Terpene” was therefore hereafter used to  
 208 designate all emitted terpenoid VOCs.

209 **Table 1. Reagent ions and specific ions used to monitor VOCs emitted from the PB.**

VOC	Formaldehyde	Acetone	Acetaldehyde	Propanal	Butanal	Pentanal	Hexanal	Terpenes
<b>Reagent ion</b>	H <sub>3</sub> O <sup>+</sup>	NO <sup>+</sup>	NO <sup>+</sup>	NO <sup>+</sup>	NO <sup>+</sup>	NO <sup>+</sup>	NO <sup>+</sup>	NO <sup>+</sup>
<b>Specific ion</b>	CH <sub>3</sub> O <sup>+</sup>	NO <sup>+</sup> .C <sub>3</sub> H <sub>6</sub> O	CH <sub>3</sub> CO <sup>+</sup>	C <sub>3</sub> H <sub>5</sub> O <sup>+</sup>	C <sub>4</sub> H <sub>7</sub> O <sup>+</sup>	C <sub>5</sub> H <sub>9</sub> O <sup>+</sup>	C <sub>6</sub> H <sub>11</sub> O <sup>+</sup>	C <sub>10</sub> H <sub>16</sub> <sup>+</sup>
<b>m/z</b>	31	57	43	57	71	85	99	136
<b>LoD (ppb)</b>	20	37	28	2	1	1	26	6

210 Before placing the PB in the experimental chamber, the chamber was flushed with fresh air,  
 211 and blank measurements were taken to determine the background VOC concentrations.  
 212 SIFT-MS VOC monitoring started as soon as the material was placed inside the experimental  
 213 chamber. An airflow rate of 25 mL.min<sup>-1</sup> was continuously sampled from the centre of the  
 214 chamber by the analytical device. The volume of gas sampled throughout emission  
 215 experiments was typically less than 6% of the volume of the experimental chamber, and thus  
 216 gas sampling was assumed not to affect the emission equilibrium.

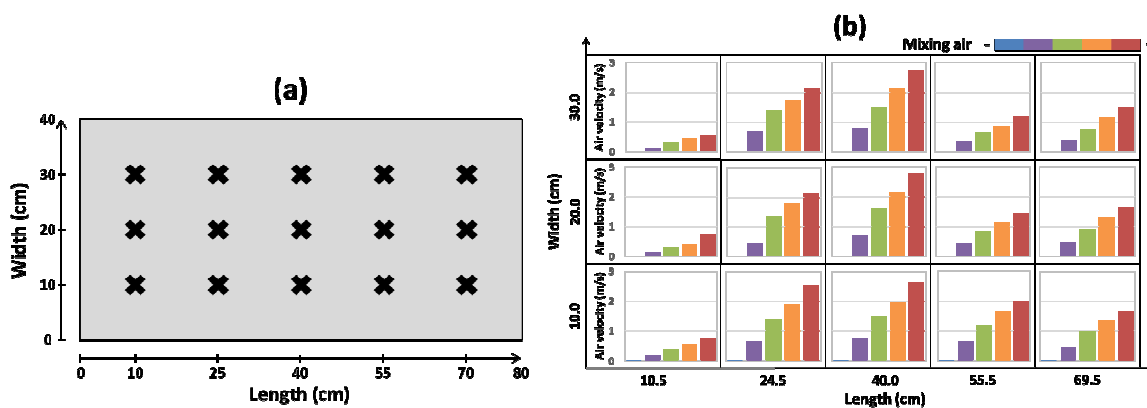
#### 217 **2.2.4. Aeraulic characterization of the chamber**

218 Ventilation can be characterized by two aspects: the ACR and the air velocity near to the  
 219 material’s surface.

220 *The ACR* corresponds to the rate at which indoor air is renewed by incoming fresh air. It is  
 221 expressed as a number of volumes per hour (h<sup>-1</sup>). The ACR in our ventilated chamber, with  
 222 an operation range of 0 - 18.75 h<sup>-1</sup>, was controlled by two BROOKS mass flow regulators.

223 *The air velocity near to the material's surface* is defined in the direction of the airflow along  
 224 the PB. Air velocity profiles near the material’s surface had to be investigated and  
 225 determined. Air velocities were measured using a TSI hot wire anemometer probe placed 0.5  
 226 cm above the surface of the PB; it had a resolution of 0.01 m.s<sup>-1</sup>. First, the airflow was

227 established inside the chamber after replacing one of the lateral sides of the chamber by a  
 228 wooden panel drilled at several points at the relevant distance from the bottom of the  
 229 chamber to allow the probe insertion. The end of the probe was oriented in the direction of  
 230 the airflow, parallel to the surface of the material to be measured. Air velocity measurements  
 231 using the anemometer probe were performed in 15 separate locations above the material's  
 232 surface as shown in Figure 2-a. The air velocity profiles determined were then used to  
 233 calculate an average air velocity at the surface of the material under various air mixing  
 234 conditions. Figure 2-b presents an example of an air velocity profile near to the material's  
 235 surface. This profile is the result of measurement of five average air velocities near to the  
 236 material's surface: 0; 0.5; 1.0; 1.4, and 1.8 m.s<sup>-1</sup>. Note that the ACR has no effect on the air  
 237 velocity over the material's surface. Consequently, only the fan used to mix the air inside the  
 238 chamber controls the air velocity over the material's surface.



239  
 240 **Figure 2. (a) Top view schematic representation of the material surface, crosses represent**  
 241 **locations where air velocity was measured, (b) example of air velocity profile near to the**  
 242 **material's surface as a function of air mixing at a constant ACR of 3.5 h<sup>-1</sup>.**

### 243 2.3. Experimental protocol for the chamber scale approach

#### 244 2.3.1. Characterizing the effect of ventilation on VOC emission rates

245 To assess the effect of ventilation, it was necessary to examine how: (i) the air velocity near  
 246 to the material's surface, and (ii) the ACR affected emission rates for the VOCs emitted from  
 247 the PB at 21 °C and 50% RH.

248 The first series of experiments assessed how the air velocity near to the material's surface  
249 affected emission rates for the main VOCs. An ACR of 4.5 h<sup>-1</sup> was set and the average air  
250 speeds over the material's surface tested were: 0; 0.5; 1.0; 1.4, and 1.8 m.s<sup>-1</sup> without  
251 changing the PB sample. The second series of tests assessed the impact of the ACR on  
252 emission rates for the main VOCs monitored. The average air velocity near to the material's  
253 surface was 0.5 m.s<sup>-1</sup>, whereas the ACR was set to: 2.5; 3.5; 4.5, or 5.5 h<sup>-1</sup>. The PB sample  
254 was changed between experiments.

255 The VOC concentration gradient between the material's surface and the ambient air was  
256 monitored over time to allow VOC emission rates to be considered and compared under  
257 equilibrated conditions. Therefore, after loading the PB into the experimental chamber,  
258 concentrations were allowed to stabilize until changes no longer exceeded the corresponding  
259 measurement uncertainty. At this stage, the VOC dynamic equilibrium between the gas-  
260 phase and the material's surface was considered have been reached. Thus, the  
261 concentration of a given VOC at the dynamic equilibrium corresponds to the steady state  
262 concentration. The emission rate was deduced from this steady state concentration for VOC  
263 *i*, the ACR and the loading factor, as described in Equation 1. The steady state concentration  
264 corresponds to the average concentration measured over 20 min at least 1 h after reaching  
265 the VOC emission equilibrium.

266  $E_i = NC_{ss,i}/L$  (Equation 1)

267 In Equation 1,  $E_i$  is the emission rate for VOC *i* (μg.m<sup>2</sup>.h<sup>-1</sup>),  $N$  is the ACR (h<sup>-1</sup>),  $C_{ss,i}$  is the  
268 steady state concentration of VOC *i* (μg.m<sup>-3</sup>) and  $L$  is the loading factor for the emissive  
269 material (m<sup>2</sup>.m<sup>-3</sup>), which corresponds to the ratio between the exposed surface area (m<sup>2</sup>) and  
270 the air volume (m<sup>3</sup>).

### 271 **2.3.2. Characterizing variability between PB samples**

272 The PB samples used for each series of tests were from the same batch, but as the  
273 manufacturing process could introduce variability between PB samples, it was nevertheless

274 necessary to assess their heterogeneity. Heterogeneity between samples was assessed  
275 based on variations in the individual VOC emission rates between three samples; it was  
276 expressed as a standard deviation value. For these purposes, three experiments were  
277 performed at 21 °C, 50% RH and at an ACR of 4.5 h<sup>-1</sup>, changing the PB sample between  
278 experiments.

### 279 **2.3.3. Characterizing VOC depletion from the PB**

280 The chosen material acts as a source of VOCs throughout the all experiments, since mass  
281 transfer for the VOC occurs continuously from the solid bulk material to the air. Under  
282 ventilated conditions, gas-phase VOC concentrations at dynamic equilibrium tended to  
283 decrease gradually as a result of VOCs present in the solid material becoming depleted over  
284 time as a result of emission, since they are present in the material in finite quantities. This  
285 process is called material depletion and can be characterized by a depletion rate,  $k_d^i$   
286 expressed in h<sup>-1</sup>.

287 Material depletion was assessed by performing a series of six consecutive, identical  
288 experiments with a single PB at an ACR of 4.5 h<sup>-1</sup> under constant temperature ( 21 °C) and  
289 RH (50%). The PB was removed from the chamber and stored under plastic film between  
290 tests while flushing the chamber with fresh air. In each consecutive experiment, the VOC  
291 concentrations were determined once the steady state had been reached. The concentration  
292 profiles obtained in these experiments could be described as an exponential decay from  
293 which the depletion rate for a given VOC  $k_d^i$  can then be determined.

### 294 **2.3.4. Characterizing the temperature effect**

295 According to Wolkoff (1998), temperature affects the emission rate for some VOCs but this  
296 temperature effect strongly depends on the type of material and the nature of the emitted  
297 VOC. According to the statistical analysis proposed by Liu et al. (2014), VOC emissions  
298 increased significantly at high temperature, as shown by the good agreement between the  
299 model-predicted concentration, based on diffusion within the solid material, and the gas-

300 phase concentration measured. In contrast, Huangfu et al. (2019) clearly highlighted a linear  
301 relationship between the formaldehyde concentration over a 20 to 45 ppb range and an  
302 indoor air temperature ranging from 19 to 24 °C.

303 Based on these observations, the influence of temperature on VOC emissions must be  
304 assessed. The effect of temperature on VOC emissions was examined in the steady state  
305 concentration regime under airtight conditions with a single material plate in conditions  
306 guarding against VOC depletion from the material, and to limit variability between samples.  
307 In these experiments, five temperatures from 19 to 28 °C were tested in a random order, by  
308 changing the temperature of the inlet air and the laboratory temperature after emissions had  
309 reached the steady state.

310 From this experimental assessment, a relationship linking VOC concentrations under airtight  
311 conditions to temperature was determined. The influence of temperature on the VOC  
312 concentrations can be then characterized by the relative concentration enhancement of VOC  
313 i per degree Celsius, as described By Equation 2.

$$\alpha_i = \frac{C_i(T_{max}) - C_i(T_{min})}{(T_{max} - T_{min})C_i(T_{ref})} \text{ (Equation 2)}$$

315 Where  $C_i$  is the concentration of VOC i at a fixed temperature (ppb),  $T_{max}$  is the maximum  
316 temperature in the range (°C), and  $T_{min}$  is the minimum temperature in the range (°C).

## 317 **2.4. Experimental protocol for the material scale approach**

### 318 **2.4.1. Principle of the experimental method used to determine the emission**

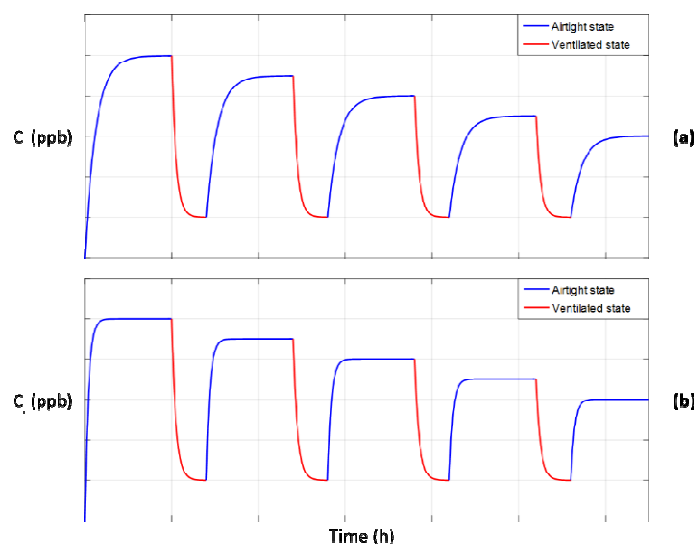
#### 319 **parameters: $K_i$ , $C_{0,i}$ & $D_i$**

320 The principle of the method proposed by Zhou et al. (2018) is based on the alternation of two  
321 states: (i) *VOC emissions monitored under airtight conditions* and, (ii) *VOC emissions*  
322 *monitored under ventilated condition.*

323 In the first step, VOCs are emitted from the solid material of interest, placed in a clean  
324 experimental chamber, under airtight conditions, constant temperature, and RH. The source

325 material is left inside the experimental chamber until the emission equilibrium is reached for  
326 every VOC. The concentration of VOC  $i$  at equilibrium in the airtight container, expressed in  
327  $\text{mg}\cdot\text{m}^{-3}$ , corresponds to the average concentration measured over 20 min at least 1 h after  
328 reaching the VOC equilibrium between the gas-phase and the material's surface. Fresh air  
329 was then introduced into the experimental chamber at a constant airflow rate, with an ACR  
330 set to  $2.35 \text{ h}^{-1}$  to mark the beginning of the second step: monitoring of VOC emissions under  
331 ventilated conditions. When all VOC concentrations in the chamber had once again reached  
332 a concentration equilibrium, the ventilated step was considered finished and the setup was  
333 returned to the airtight condition. The solid material was subjected to a total of five airtight  
334 conditions and four ventilated conditions as reported in Figure 3. To assess the repeatability  
335 of this experimental method, three full experimental sequences were performed under the  
336 same experimental conditions.

337 As illustrated in Figure 3, different VOCs emitted from the same material may exhibit distinct  
338 individual emission kinetics, especially under airtight conditions. Some VOCs can reach their  
339 steady state equilibrium within only 3-4 h, while others may need more than 10 h. These  
340 contrasting emission kinetics generate a time constraint when establishing the steady state in  
341 each experimental phase for all VOCs. Therefore, it was necessary to wait at least 10 h  
342 under airtight conditions to ensure that all VOCs had reached their respective steady states.  
343 The steady state for a given VOC is reached when the measured concentration of that VOC  
344 does not vary beyond its measurement uncertainty for a minimum of 20 min.



345  
 346 **Figure 3. Theoretical plots of the successive emission states: (a) gas concentration (ppb) of**  
 347 **VOC i illustrating a slow kinetic emission as a function of time; (b) gas concentration (ppb) of**  
 348 **VOC j illustrating a rapid kinetic emission as a function of time.**

349 During the ventilated phases, the nature of the VOCs did not significantly influence the time  
 350 required to reach the steady state because fresh air was constantly passing through the  
 351 system. To ensure all VOCs have reached their steady state, it was necessary to wait from 4  
 352 to 5 h under ventilated conditions. Note that the VOC concentration was considered to be at  
 353 the steady state if it remained unchanged beyond the measurement uncertainty for at least  
 354 one hour.

#### 355 **2.4.2. Determining $K_i$ and $C_{0,i}$ from experimental data by linear fitting**

356 After performing the multiple airtight and ventilated protocols, the concentration of VOC i  
 357 reached at equilibrium during each airtight step and the total mass of VOC i emitted during  
 358 ventilated periods were determined from the temporal concentration profiles for each VOC  
 359 (Figure 3). For each ventilated state, the mass of VOC i emitted, expressed in mg, was  
 360 calculated using the trapezoidal quadrature formulae.

361 Henry's law describes the transient and reversible equilibrium relationship between the gas  
 362 phase concentration at equilibrium and the adsorbed phase concentration on the solid  
 363 material. Based on this law, the general VOC mass balance inside the chamber for the

364 multiple airtight/ventilated emission states was used to develop the relationship between the  
365 VOC concentration at equilibrium and the mass of VOC emitted, including the partitioning  
366 coefficient and the initial emittable concentration. The general mass balance equation can be  
367 found in original publication of Zhou et al. (2018). Finally, the partitioning coefficient  $K_i$  and  
368 the initial emittable concentration  $C_{0,i}$  were obtained for VOC  $i$  from the linear fitting of  
369 multiple sets of VOC concentrations at equilibrium, and the mass of VOC  $i$  emitted.

### 370 **2.4.3. Determining $D_i$ by solving analytical equations**

371 In addition to  $K_i$  and  $C_{0,i}$ , the diffusion coefficient  $D_i$ , expressed in  $m^2 \cdot s^{-1}$ , must be determined  
372 for VOC  $i$ . This parameter is calculated by non-linear fitting of the first experimental curve for  
373 airtight emission and analytical resolution of the equation of gas-phase VOC concentrations  
374 in an airtight chamber using the  $K_i$  and  $C_{0,i}$  values determined previously, as proposed by  
375 Xiong et al. (2011).

376 When characterizing the mass transfer for VOC  $i$ , the Biot number is included in the equation  
377 of the gas-phase VOC concentration in an airtight chamber. The Biot number corresponds to  
378 the ratio between the mass transfer inside the material and the mass transfer at the  
379 material's surface; therefore, the convective mass transfer coefficient  $h_i$  through the boundary  
380 layer at the surface-air interface for each VOC  $i$ , expressed in  $m \cdot s^{-1}$ , is included in the  
381 equation. According to Axley (1991), the convective mass transfer coefficient  $h_i$  for VOC  $i$  can  
382 be theoretically calculated by applying Equation 3. This equation includes the Reynolds  
383 number and the Schmidt number, described by Equation 4 and Equation 5, respectively.

$$384 \frac{h_i L}{\delta_i} = 0.664 Re^{1/2} Sc^{1/3} \quad (\text{Equation 3})$$

385 For  $Re < 500,000$

$$386 Re = \frac{UL}{\nu} \quad (\text{Equation 4})$$

$$387 Sc = \frac{\nu}{\delta_i} \quad (\text{Equation 5})$$

388 Where  $Re$  is the Reynolds number,  $Sc$  is the Schmidt number,  $\delta_i$  is the molecular diffusivity  
389 of VOC  $i$  in air outside the boundary layer ( $m^2.s^{-1}$ ),  $U$  is the mean air velocity outside the  
390 boundary layer ( $m.s^{-1}$ ),  $L$  is the length of the surface in the direction of airflow (m) and  $\nu$  is the  
391 kinetic viscosity of the air phase ( $m^2.s^{-1}$ ).

#### 392 **2.4.4. Method to estimate the molecular diffusivity of VOC $i$ in air**

393 Calculation of the convective mass transfer coefficient,  $h_i$ , for VOC  $i$  depends on the  
394 experimental conditions and on the molecular diffusivity coefficient of VOC  $i$ . This value must  
395 therefore be individually determined for each VOC. However, molecular diffusivity coefficient  
396 values were found for five VOCs in the GSI chemical database, except for pentanal, hexanal,  
397 and terpenes. Among the chemical property estimation methods present in the literature, the  
398 method proposed by Fuller et al. (1969) can be used to estimate the molecular diffusivity  
399 coefficient of a binary gas-phase system based on the molar weight and the atomic diffusion  
400 volume (Fuller et al., 1969, 1966; Fuller and Giddings, 1965). Based on an empirical  
401 relationship proposed by Fuller et al. (1969), Equation 6 was modified to estimate the  
402 molecular diffusivity coefficient  $\delta_i$  for a given VOC  $i$  in air.

$$403 \delta_i = \frac{0.01 T^{1.75} (1/M_i + 1/M_{air})^{1/2}}{P \left[ (\sum v)_i^{1/3} + (\sum v)_{air}^{1/3} \right]^2} \text{ (Equation 6)}$$

404 In Equation 6,  $\delta_i$  is the molecular diffusivity coefficient of VOC  $i$  in air ( $m^2.s^{-1}$ ),  $T$  is the  
405 temperature (K),  $P$  is the pressure (Pa),  $M_i$  is the molar weight of VOC  $i$  ( $g.mol^{-1}$ ),  $M_{air}$  is the  
406 molar weight of air ( $g.mol^{-1}$ ) and  $\sum v$  is the sum of atomic diffusion volume increments ( $cm^3$ ).  
407 The atomic diffusion volume increments were determined by performing regression analysis  
408 on extensive experimental data and are reported in Fuller et al. (1969).

### 409 **3. Results and discussion**

410 The following sections present the results of the study split into two main parts. The first part  
411 focuses on the chamber scale investigation with the prior assessment of VOC emission  
412 variability and the assessment of the influence of ventilation on VOC emissions. The second

413 part focuses on the material scale investigation, presenting the emission parameters  
414 describing the VOC mass transfer.

### 415 **3.1. Chamber scale investigation**

#### 416 **3.1.1. Assessing emission variability**

417 Before assessing the influence of ventilation on VOC emissions, it was necessary to  
418 determine the variability of VOC emissions, including (i) variability between samples, (ii)  
419 depletion of VOC from the material studied, and (iii) the influence of temperature on VOC  
420 emissions.

#### 421 **3.1.2. Variability of emission rates between samples**

422 Emission variability was assessed by determining the standard deviation of the emission  
423 rates measured for three PB samples. For every VOC monitored and for the three PB  
424 samples, Table 2 lists the emission rates followed by the measurement uncertainties. The  
425 standard deviation related to the variability of the emission rate between samples was  
426 calculated for all VOCs.

427 **Table 2. Emission rates of VOCs ( $\mu\text{g}\cdot\text{m}^{-2}\cdot\text{h}^{-1}$ ) and associated standard deviations (SD)**  
428 **determined from three series of experiments performed under the same conditions.**  
429 **Uncertainties correspond to the SD calculated from the concentrations measured.**

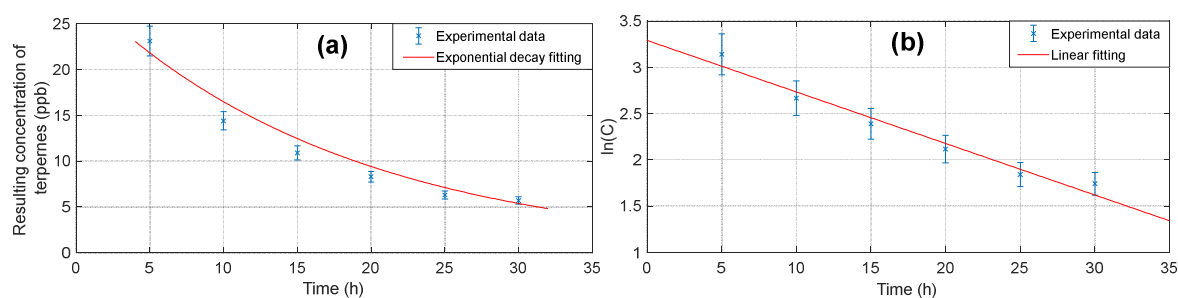
$E_i$ ( $\mu\text{g}\cdot\text{m}^{-2}\cdot\text{h}^{-1}$ )	Formaldehyde	Acetone	Acetaldehyde	Propanal	Butanal	Pentanal	Hexanal	Terpenes
<b>Sample 1</b>	223 ± 12	2887 ± 170	125 ± 14	18.3 ± 1.7	8.0 ± 1.0	17.0 ± 1.4	1082 ± 58	226 ± 16
<b>Sample 2</b>	256 ± 14	3265 ± 193	141 ± 16	17.2 ± 1.6	8.0 ± 1.0	19.0 ± 1.5	1248 ± 67	305 ± 21
<b>Sample 3</b>	234 ± 13	3214 ± 190	133 ± 15	17.2 ± 1.6	8.0 ± 1.0	19.0 ± 1.5	1209 ± 65	348 ± 24
<b>SD</b>	16.9	205.1	7.7	0.6	0.1	1.1	86.8	62.3

430 As reported in Table 2, the SD reflecting the variability of emission rates between PB  
431 samples from the same batch were less than 8%, except for terpenes, which has a 21.3%  
432 SD. The SD for formaldehyde, acetone, terpenes, and hexanal were all higher than the  
433 corresponding measurement uncertainties. The amounts of these VOCs present in the PB  
434 samples from the same batch presented a slight variability between samples. SD for  
435 acetaldehyde, propanal, butanal, and pentanal were lower than the measurement

436 uncertainties. The amounts of these VOCs into the PB samples can therefore be regarded as  
437 homogeneous.

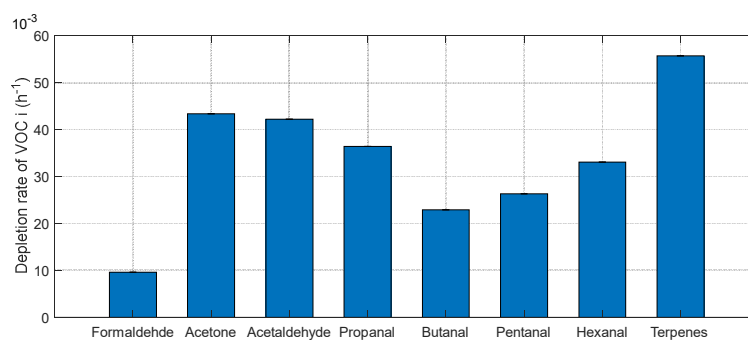
### 438 3.1.3. Contribution of natural depletion

439 The characterization of VOC depletion from the material based on a series of six consecutive  
440 experiments on a single PB under identical experimental conditions is illustrated by the  
441 terpene concentration plotted over time, i.e. the depletion profile for terpenes, shown in  
442 Figure 4.



443  
444 **Figure 4. (a) Terpene depletion profile determined from six consecutive experiments. (b)**  
445 **Linearized depletion profile for terpene. Uncertainties correspond to the standard deviation**  
446 **calculated from the concentrations measured. ( $T = 21 \pm 0.5$  °C,  $RH = 50 \pm 5\%$ ,  $ACR = 4.5$  h<sup>-1</sup>,**  
447 **surface air velocity = 0.5 m.s<sup>-1</sup>).**

448 Like this terpene depletion profile (Figure 4-a), all monitored VOCs followed an exponential  
449 decay profile that could be described with first order kinetics. These temporal profiles are in  
450 agreement with findings reported by Harb et al. (2018). Depletion rates expressed in h<sup>-1</sup>,  
451 were retrieved, for each VOC from the slope of the linearized temporal profiles (Figure 4-b).



452  
453 **Figure 5. Depletion rates for the eight VOCs monitored in the selected PB (h<sup>-1</sup>).**

454 All VOCs were characterized by depletion rates within the same order of magnitude (Figure  
455 5). The lowest value was recorded for formaldehyde at  $9.6 \times 10^{-3} \text{ h}^{-1}$ , whereas other VOCs  
456 presented depletion rates exceeding  $22.9 \times 10^{-3} \text{ h}^{-1}$ . Considering the depletion rates  
457 measured for all VOCs, the VOC depletion of the PB is less than 2% over the 20 min  
458 required to determine the steady state concentration.

459 The depletion rates reported here are one order of magnitude higher than those reported in  
460 Harb et al. (2018). This apparent discrepancy is probably mainly linked to differences in  
461 ventilation conditions. Indeed, we used an ACR of  $4.5 \text{ h}^{-1}$  in our experiments; whereas Harb  
462 et al. (2018) used a lower ACR of  $0.3 \text{ h}^{-1}$ . The flushing of the air volume by the higher ACR  
463 increases the concentration gradient between the material's surface and the air. Therefore,  
464 with a higher ACR, mass transfer of VOC from the material to the air increases due to the  
465 larger concentration gradient, and consequently the VOC is more rapidly depleted from the  
466 material.

467 As the material depletion was significant over the timespan of the experiments investigating  
468 the influence of ventilation on VOC emission rates, the VOC concentration profiles obtained  
469 should be corrected using the depletion rate determined as detailed in Harb et al. (2018),  
470 using Equation 7.

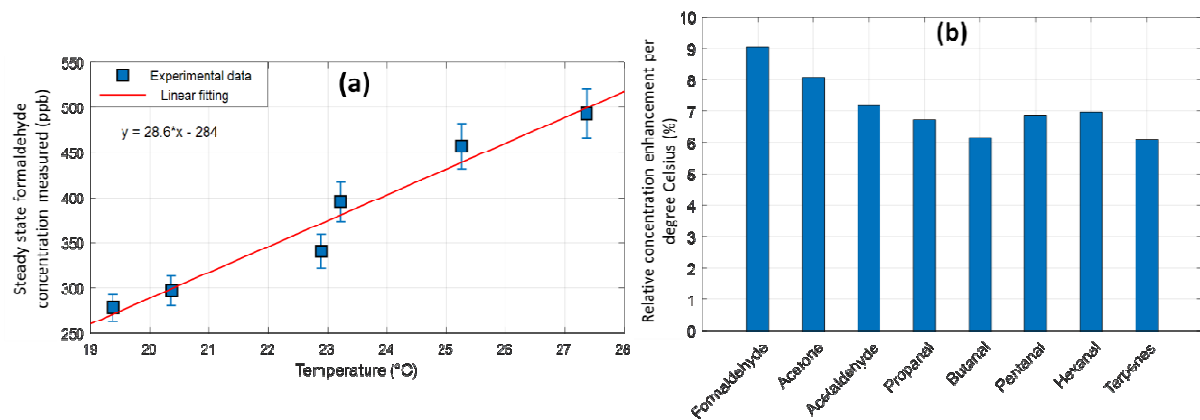
471 
$$C_{corr}^i = \exp[\ln(C^i) + (k_d^i t)] \text{ (Equation 7)}$$

472 Where  $C_{corr}^i$  is the corrected VOC i concentration (ppb),  $C^i$  is the measured VOC i  
473 concentration (ppb),  $k_d^i$  is the depletion rate for VOC i ( $\text{h}^{-1}$ ) and  $t$  is the time along the  
474 consecutive series of experiments (h).

#### 475 **3.1.4. Effect of temperature on VOC concentrations**

476 The effects of temperature on the concentration of a given VOC are illustrated in Figure 6-a  
477 for formaldehyde. Uncertainties correspond to the SD calculated from the monitoring of

478 steady state concentrations. For each VOC, Figure 6-b shows the relative concentration  
479 enhancement per degree Celsius.



480  
481 **Figure 6. (a) Steady state concentration of formaldehyde (ppb) as a function of chamber**  
482 **temperature (°C); (b) Relative concentration enhancement per degree Celsius (%) for each**  
483 **VOC monitored.**

484 As illustrated in Figure 6-a for formaldehyde, all VOCs presented a linear relationship  
485 between their steady state concentrations and the temperature in the chamber under airtight  
486 conditions over the temperatures range 19 to 28 °C. The sensitivity of VOC concentrations to  
487 temperature is represented by the relative concentration enhancement per degree.  
488 According to Figure 6-b, all VOCs were temperature-sensitive, with relative concentration  
489 enhancements between 6 and 9 %.

490 The sensitivity of VOC emissions to temperature underscores the need to consider this  
491 parameter when setting up experimental tests, especially under unstable temperature  
492 conditions. From the relative concentration enhancement parameter (Equation 2), the  
493 concentration datasets can be corrected for temperature when the temperature fluctuates  
494 during experiments. However, it is not always necessary to correct data with respect to  
495 temperature, and VOC concentrations should only be corrected when large temperature  
496 variations occur, particularly in long-term experiments.

497 According to the literature, the effect of RH on VOC emissions does not show any particular  
498 trends. Indeed, authors report a variable influence of RH on VOC emissions depending on

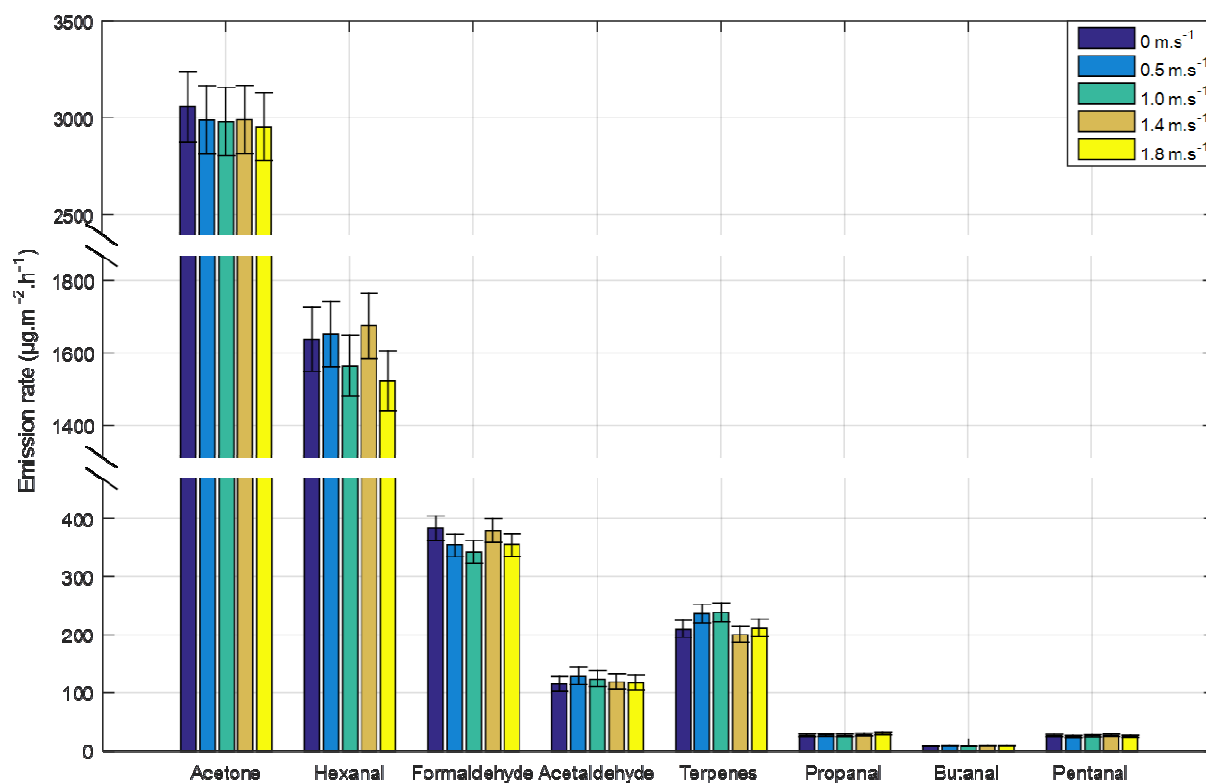
499 the VOC-material system considered (Colombo et al., 1993; L. Huang et al., 2013; Wolkoff,  
500 1998). When studying VOC emissions at different RH conditions, it appears required that  
501 selected materials undergo preliminary conditioning at the targeted RH to equilibrate the  
502 material surface and bulk to the corresponding RH before initiating any test. This preparation  
503 aims to avoid material absorption/release of moisture and maintain constant RH along  
504 experimental tests. Evaluating the effect of RH is complex since the material preparation may  
505 induce VOC depletion resulting in VOC emissions from the material. During experiments,  
506 variations in RH may affect the emission data obtained. Therefore, along our experiments,  
507 the RH remains constant in order not to bias any emission process.

### 508 **3.1.5. Influence of ventilation on VOC emission rates**

509 The chamber scale approach allowed us to study the effect of ventilation on VOC emission  
510 rates from the selected PB. The roles of air velocity over the material's surface and ACR  
511 were dissociated. Their respective influence on VOC emission rates were investigated and  
512 are reported in this section.

### 513 **3.1.6. Specific influence of air velocity over the material surface on VOC** 514 **emission rates**

515 The impact of changes in the air velocity near to the material's surface on VOC emissions  
516 from PB was studied by determining the emission rates for VOCs when applying different air  
517 velocities over the material's surface at a constant ACR. The corresponding data are  
518 reported in Figure 7. Since a single material sample was used for this series of tests,  
519 datasets were corrected to account for VOC depletion, assuming a constant depletion rate  
520 over the series of tests.



521  
 522 **Figure 7. Emission rates ( $\mu\text{g}\cdot\text{m}^{-2}\cdot\text{h}^{-1}$ ) for the eight main VOCs when applying different air**  
 523 **velocities near to the material's surface ( $\text{m}\cdot\text{s}^{-1}$ ). Uncertainties correspond to the standard**  
 524 **deviation calculated from the steady state concentrations measured.**

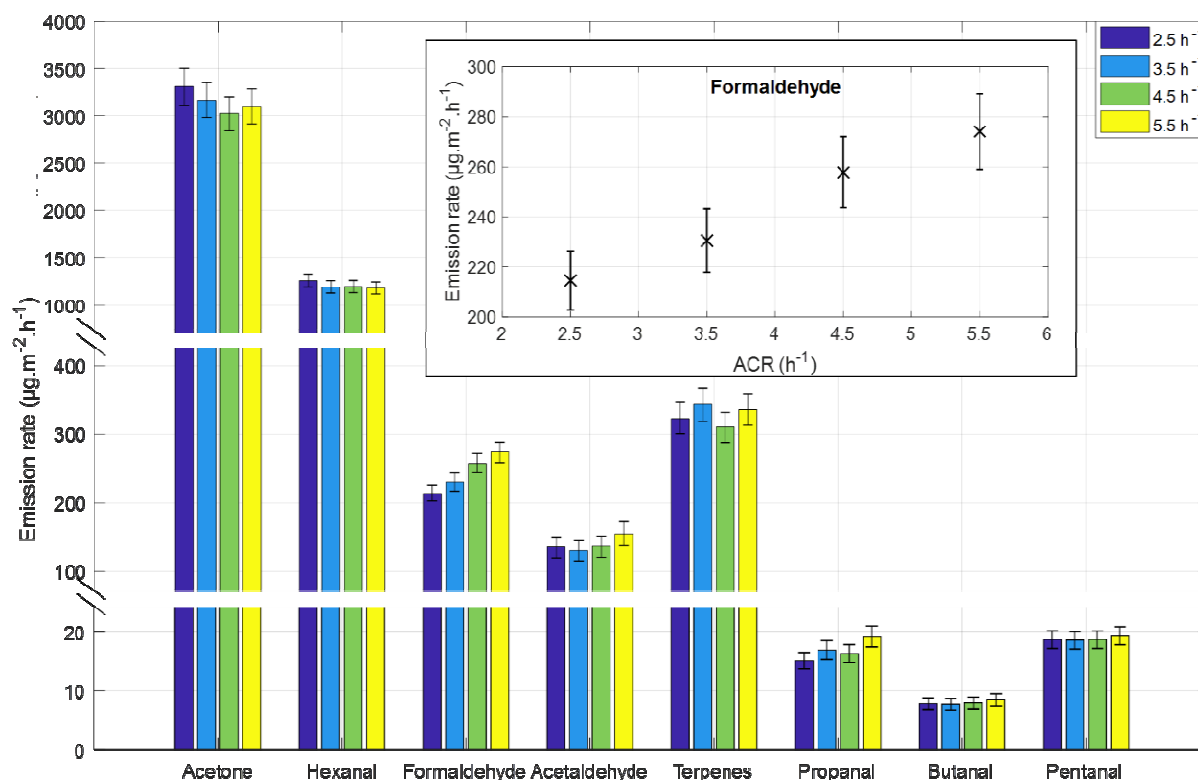
525 Among the VOCs monitored, acetone, hexanal and formaldehyde presented the highest  
 526 emission rates, with values exceeding  $280 \mu\text{g}\cdot\text{m}^{-2}\cdot\text{h}^{-1}$ ; the emission rates for other VOCs  
 527 were less than  $75 \mu\text{g}\cdot\text{m}^{-2}\cdot\text{h}^{-1}$ . According to our data (Figure 7), the air velocity over the PB  
 528 surface did not significantly affect emission rates for the eight VOCs monitored.

529 In contrast to these results, some publications, such as Hun et al. (2010), suggested that the  
 530 air velocity over the material's surface could affect VOC emission. An increase in the air  
 531 velocity would have affected VOC emissions if they were mainly controlled by the convective  
 532 mass transfer across the boundary layer (Knudsen et al., 1999). The VOC emissions  
 533 measured here with the selected PB can hence be considered mainly influence by diffusion  
 534 within the solid material. The VOC emission from the solid materials has a variable sensitivity  
 535 to the air velocity over the material's surface depending on the predominant mechanism  
 536 specific to each VOC-material pair.

537

### 3.1.7. Specific influence of the ACR on VOC emission rates

538 The influence of the ACR on VOC emissions from PB is illustrated in Figure 8. The emission  
539 rates for VOCs were measured in the chamber under different ACR while applying a  
540 constant air velocity over the material's surface.



541

542 **Figure 8. Emission rate ( $\mu\text{g.m}^{-2}.\text{h}^{-1}$ ) for the eight main VOCs under different ACR ( $\text{h}^{-1}$ )**  
543 **conditions. Inset: emission rates for formaldehyde as a function of the ACR. Uncertainties**  
544 **correspond to the standard deviation calculated from the steady state concentrations**  
545 **measured.**

546 As reported in Figure 8, the emission rates for seven VOCs were not significantly affected by  
547 changes to the ACR. In contrast, the formaldehyde emission rate increased by 28 % when  
548 the ACR varies from 2.5 to 5.5 h<sup>-1</sup> that is significantly different compared to the variability  
549 between samples (7.1%). Propanal emission rates also showed a slight tendency to increase  
550 with the ACR, but overall emission rates remained lower than most other VOCs (< 20  
551  $\mu\text{g.m}^{-2}.\text{h}^{-1}$ ). These results highlight the singular behaviour of formaldehyde regarding the  
552 ACR. An increase in ACR means that more fresh air is brought into the chamber. Since the

553 air velocity close to the emissive material was constant, this should create a stronger  
554 concentration gradient across the boundary layer (Offermann and Hodgson, 2011).

555 As discussed above, the influence of air velocity on VOC emission rates suggests that VOC  
556 emissions from the selected PB, for the VOCs monitored, is mainly driven by their diffusion  
557 within the solid material. Unlike the other VOCs, formaldehyde emission was enhanced by  
558 increasing the concentration gradient from the material to the gas-phase, suggesting that  
559 formaldehyde emission is not limited by its diffusion in the material.

560 Indeed, in addition to diffusing within the material, formaldehyde may be generated by  
561 hydrolysis of the PB binder, which could explain its enhanced emission rate as the ACR  
562 increases. Most composite wood panels are known sources of formaldehyde, as they are  
563 bonded with urea-formaldehyde (UF) resins (Kelly et al., 1999; Salthammer et al., 2010).  
564 These resins have a low resistance to hydrolysis (Dunky, 1998; Salthammer et al., 2010) as  
565 a result of the reversibility of the reaction between urea and formaldehyde (Dorieh et al.,  
566 2019). Thus, the C-N bond in UF resins can be hydrolyzed in the presence of water vapour  
567 (Salthammer et al., 2010). This chemical process results in the release of free formaldehyde  
568 which contributes to the total formaldehyde emission from composite wood panels (He et al.,  
569 2019). Moreover, He et al. (2019) report that binder hydrolysis to produce formaldehyde  
570 emission increases over time, becoming the predominant source of long-term emissions. In  
571 our experiments, the supply of humid fresh air appears to promote the hydrolysis of the  
572 binder and the formation of formaldehyde. However, the contribution of this process should  
573 be limited in our conditions, since the emission phenomena are regarded as short-term.

### 574 **3.2. Material scale investigation**

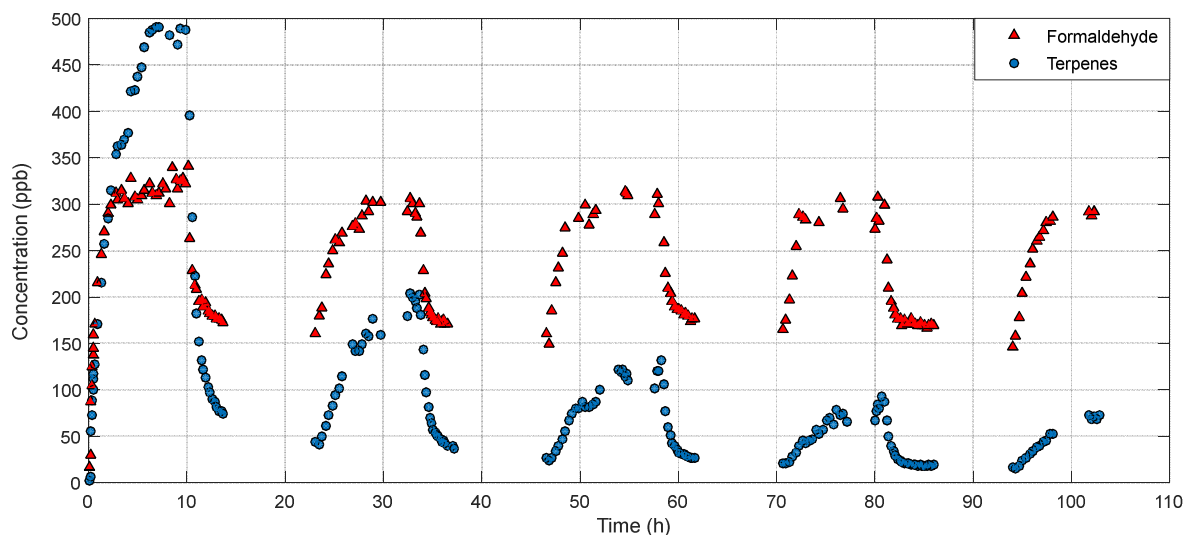
575 In contrast to the previous series of tests, each experimental protocol alternately analysing  
576 airtight/ventilated emission lasted for a full week. Over the course of these experiments,  
577 temperature varied in line with day-night cycles, with fluctuations from 20 to 25 °C. Maximum  
578 temperatures were measured during the day due to sunlight.

579 To account for these variations, a data correction was applied to concentration profiles using  
580 Equation 8, considering an identical influence of temperature on VOC emission in both  
581 steady state and transient conditions.

$$582 \quad C_{corr,i} = C_{exp,i} + \alpha_i C_{exp,i} (T_{ref} - T_{exp}) \text{ (Equation 8)}$$

583 In Equation 8,  $C_{corr,i}$  is the temperature corrected concentration (ppb) of VOC  $i$ ,  $C_{exp,i}$  is the  
584 experimental concentration (ppb) of VOC  $i$ ,  $T_{ref}$  is the reference temperature set at 21 °C,  $T_{exp}$   
585 is the experimental temperature and  $\alpha_i$  is the relative concentration enhancement of VOC  $i$   
586 per degree Celsius, as described in Equation 2. Concentration profiles for VOCs were  
587 corrected for temperature variations using Equation 2 and Equation 8, setting a reference  
588 temperature of 21 °C.

589 After performing the airtight/ventilated alternately emission experiments, corrected VOC  
590 concentrations were plotted. Figure 9 shows the examples of terpenes and formaldehyde. In  
591 this figure, the terpene concentration dynamic illustrates the behaviour of all targeted VOCs  
592 except formaldehyde, which was therefore represented separately.



593  
594 **Figure 9. Comparison of the experimental concentration profiles for formaldehyde and**  
595 **terpenes (representing all other VOCs) (ppb).**

596 All the experimental concentration profiles for VOCs were in agreement with the theoretical  
597 profiles shown in Figure 3. Figure 9 reveals two types of individual behaviour characterizing  
598 so-called 'rapid' and 'slow' kinetics, illustrated by formaldehyde and terpenes, respectively.

599 With the exception of formaldehyde, all VOCs presented similar emission kinetics, with from  
600 5 to 15 h required to reach the steady state under airtight conditions. In addition, when  
601 switching from the airtight to the ventilated regime, a sharp decrease in concentration was  
602 observed with an average concentration drop exceeding 80% between the two regimes. The  
603 steady state concentration of terpenes under airtight conditions decreased from 490 to 75  
604 ppb within less than 4 h of switching from the airtight to the ventilated condition.

605 In contrast, the concentration difference for formaldehyde between the airtight and ventilated  
606 regimes was lower than for other VOCs, with an average concentration drop of 45%.  
607 Noticeably, under ventilated conditions, formaldehyde maintained a concentration of ca. 175  
608 ppb throughout the experimental sequence. Similarly, under the airtight regime, the steady  
609 state concentrations of formaldehyde were equivalent from one series of measurements to  
610 the next. In contrast, the steady state concentrations of other VOCs gradually decreased as  
611 time progressed.

612 Thus, compared to other VOCs, formaldehyde presents a singular behaviour in response to  
613 the ventilation regimes tested. This behaviour is in line with the results from the chamber  
614 scale approach. These findings suggest that the mechanisms driving formaldehyde emission  
615 could be quite different to those driving emission of the other VOCs monitored, as discussed  
616 above in relation to binder hydrolysis.

### 617 **3.2.1. Determining $K_i$ and $C_{0,i}$ by linear fitting**

618 To determine the partitioning coefficient  $K_i$  and the initial emittable concentration  $C_{0,i}$ , the  
619 experimental data for the three experiments was fitted with a linear function. Experimental  
620 partitioning coefficients are reported in Table 3; Table 4 lists initial emittable concentrations.

621 Uncertainties correspond to the standard deviation (SD) calculated from the three  
622 independent experiments.

623 **Table 3. Partitioning coefficient  $K_i$  of VOCs and associated standard deviation (SD) determined**  
624 **from three experiments performed under the same conditions.**

$K_i$	Formaldehyde	Acetone	Acetaldehyde	Propanal	Butanal	Pentanal	Hexanal	Terpenes
<b>Experiment 1</b>	4380	211	180	193	312	273	313	113
<b>Experiment 2</b>	4404	212	180	206	355	317	316	109
<b>Experiment 3</b>	3184	225	198	267	357	305	287	110
<b>SD (%)</b>	17.5	3.7	5.6	17.8	7.5	7.5	5.3	2.1

625 All VOCs except formaldehyde had partitioning coefficients within the same order of  
626 magnitude. A considerably higher partitioning coefficient was measured for formaldehyde.  
627 Depending on the nature of the VOC, published values for the partitioning coefficients  $K_i$   
628 varied from one hundred to several thousand (Xu and Zhang, 2011; Zhou et al., 2018).  
629 However, the partitioning coefficient values for formaldehyde presented here are consistent  
630 with results reported elsewhere (S. Huang et al., 2013; Xu and Zhang, 2011; Zhou et al.,  
631 2018).

632 For most of the VOCs investigated, uncertainties related to the partitioning coefficient were  
633 lower than 7.5%. Thus, acetone, acetaldehyde, hexanal, and terpenes had a lower SD than  
634 the corresponding measurement uncertainties, and uncertainties related to the variability  
635 between samples. Consequently, the partitioning coefficients determined for these VOCs are  
636 replicable. In contrast, the SD for butanal and pentanal were higher than the uncertainties  
637 related to the variability between samples, but lower than their measurement uncertainties.  
638 The uncertainties associated with the determination of their partitioning coefficients for these  
639 VOCs are thus mostly related to analytical uncertainties.

640 Among the VOCs monitored, formaldehyde and propanal were the most variable compounds  
641 with respective uncertainties of 17.5 and 17.8%. Nonetheless, these uncertainties remain  
642 within the acceptable range.

643 Analysis of VOC depletion from the selected PB, characterized by the depletion rates,  
 644 revealed that it tended to decrease when the partitioning coefficient increased. Thus,  
 645 formaldehyde presented the highest partitioning coefficients (>3000) and the lowest depletion  
 646 rate compared to other VOCs, and conversely, VOCs which had low partitioning coefficients  
 647 (100 – 225), such as acetone, acetaldehyde, and terpenes, presented the highest depletion  
 648 rates.

649 Under ventilated conditions, the continuous flushing of the air volume eliminates gas-phase  
 650 VOC from the chamber, which sustains the VOC mass transfer from the material to the air,  
 651 controlled by the partitioning coefficient  $K_i$ . VOC depletion thus occurs, leading to a gradual  
 652 decrease in the concentration of the compound as the emission process progresses. For  
 653 compounds with a high  $K_i$ , such as formaldehyde, the relative concentration difference  
 654 between the air and the material is also high. Consequently, the amount of VOC removed  
 655 from the air of the chamber is low compared to the amount of VOC present within the PB,  
 656 which implies a limited depletion phenomenon and a low depletion rate. In contrast, for  
 657 compounds with a low  $K_i$ , the relative concentration difference between the air and the  
 658 material is also low. In these cases, the amount of VOC eliminated with the air from the  
 659 chamber is significant compared to the amount of VOC contained in the PB, resulting in  
 660 notable depletion and a high depletion rate.

661 **Table 4. Initial emittable concentration  $C_{0,i}$  ( $\text{mg}\cdot\text{m}^{-3}$ ) of VOCs and associated standard deviation**  
 662 **(SD) determined from the three series of experiments performed under the same conditions.**

$C_{0,i}$	Formaldehyde	Acetone	Acetaldehyde	Propanal	Butanal	Pentanal	Hexanal	Terpenes
<b>Experiment 1</b>	1545	2484	105	22.6	12.4	33.7	2261	354
<b>Experiment 2</b>	1729	3188	127	28.2	15.9	43.6	2611	409
<b>Experiment 3</b>	1257	3988	119	21.1	14.7	40.5	2270	411
<b>SD (%)</b>	15.7	23.4	9.3	15.6	12.3	12.8	8.4	8.3

663 Formaldehyde, acetone and hexanal had the highest initial emittable concentrations in our  
 664 sample  $C_{0,i}$  (>1200  $\text{mg}\cdot\text{m}^{-3}$ ), whereas other VOCs presented  $C_{0,i}$  of less than 420  $\text{mg}\cdot\text{m}^{-3}$ . Our  
 665 initial emittable concentrations  $C_{0,i}$  agree with literature data (S. Huang et al., 2013; Zhou et

666 al., 2018). However, it should be noted that literature data for  $C_{0,i}$  are spread over very broad  
 667 ranges, since the initial emittable concentration depends on the type of material and its  
 668 history. History of material correspond to combination of events occurring, storage duration  
 669 and environmental conditions to which materials are subjected between manufacture and  
 670 acquisition. For instance, formaldehyde presents an average initial emittable concentration of  
 671  $17,000 \text{ mg.m}^{-3}$  with an SD of 100% for different building materials (S. Huang et al., 2013;  
 672 Zhou et al., 2018). Although the VOCs monitored presented uncertainties related to the  
 673 determination of  $C_{0,i}$  that were higher than those for the partitioning coefficient  $K_i$ , their  
 674 respective uncertainties remained less than 23.4 %.

### 675 3.2.2. Determining $D_i$ by solving of analytical equations

676 After determining  $K_i$  and  $C_{0,i}$ , the diffusion coefficient  $D_i$  was calculated by solving the  
 677 analytical equation for the gas-phase VOC concentration in the airtight mode (Xiong et al.,  
 678 2011). The VOC diffusion coefficients within the solid material  $D_i$  were determined by fitting  
 679 the result of the solution of the analytical equation and the first experimental concentration  
 680 profile under airtight conditions. VOC diffusion coefficients  $D_i$  determined from each  
 681 experiment are reported in Table 5.

682 **Table 5. Diffusion coefficients  $D_i$  ( $\text{m}^2.\text{s}^{-1}$ ) for VOCs determined from the three experiments**  
 683 **performed under the same conditions.**

$D_i$ ( $\text{m}^2.\text{s}^{-1}$ )	Formaldehyde	Acetone	Acetaldehyde	Propanal	Butanal	Pentanal	Hexanal	Terpenes
<b>Experiment 1</b>	$2.5 \times 10^{-8}$	$3.0 \times 10^{-9}$	$5.0 \times 10^{-9}$	$2.0 \times 10^{-9}$	$1.5 \times 10^{-9}$	$1.5 \times 10^{-9}$	$3.0 \times 10^{-9}$	$8.0 \times 10^{-8}$
<b>Experiment 2</b>	$2.5 \times 10^{-8}$	$3.0 \times 10^{-9}$	$4.0 \times 10^{-9}$	$3.0 \times 10^{-9}$	$1.0 \times 10^{-9}$	$1.5 \times 10^{-9}$	$3.0 \times 10^{-9}$	$5.0 \times 10^{-8}$
<b>Experiment 3</b>	$3.0 \times 10^{-8}$	$1.5 \times 10^{-9}$	$2.0 \times 10^{-9}$	$1.5 \times 10^{-9}$	$1.0 \times 10^{-9}$	$1.0 \times 10^{-9}$	$1.0 \times 10^{-9}$	$2.0 \times 10^{-9}$
<b>SD (%)</b>	10.8	34.6	41.7	35.3	24.7	21.7	49.5	89.4

684 VOC diffusion within the solid material depends on the porosity of the material and on the  
 685 nature of the given VOC. The extensive diversity of building materials studied in the literature  
 686 results in  $D_i$  values ranging from  $1.0 \times 10^{-10}$  to  $1.0 \times 10^{-6} \text{ m}^2.\text{s}^{-1}$  (S. Huang et al., 2013; Xu and  
 687 Zhang, 2011). According to the results presented in Table 6, formaldehyde had the highest  
 688 diffusion coefficient, with values ranging from  $2.5 \times 10^{-8}$  to  $3.0 \times 10^{-8} \text{ m}^2.\text{s}^{-1}$ , which is in

689 agreement with published data (Xiong et al., 2008). The diffusion coefficients determined for  
690 other VOCs varied from  $1.0 \times 10^{-9}$  to  $5.0 \times 10^{-9} \text{ m}^2 \cdot \text{s}^{-1}$ .

691 Apart from terpenes, for which variable diffusion coefficient values were measured, with an  
692 SD of 89.4%, the diffusion coefficients measured in the three experiments for all VOCs were  
693 quite similar, with SD of less than 49.5%. The results for terpenes could be explained by their  
694 higher variability between PB samples compared to other VOCs. Indeed, variations in  
695 terpene emission rates between PB samples would significantly affect the first concentration  
696 profile under the airtight conditions used to determine the diffusion coefficient  $D_i$ , resulting in  
697 more scattered diffusion coefficient values for terpenes.

698 According to the data presented in Table 5, formaldehyde once again differs from the other  
699 VOCs monitored. Based on the results of this study, the enhanced formaldehyde emission  
700 rate as a function of the ACR could be explained by the following three hypotheses: (i)  
701 Subject to the dynamic equilibrium concentration between the material and the air, the VOC  
702 mass transfer needs to be strengthened if we are to satisfy this balance when the ACR  
703 increases. As VOC emissions from the PB appears to be mainly driven by their diffusion  
704 within the solid material, the diffusion process must contribute to formaldehyde emission  
705 differently compared to the other VOCs monitored. In the case of formaldehyde, its high  
706 diffusion within the material allows a continuous supply to reach the material's surface. In  
707 contrast, the material's surface is less supplied with other VOCs due to their slower diffusion  
708 within the solid material. Given the low rate of transport of VOCs to the material's surface by  
709 diffusion, the amount of VOCs emitted from the material-air interface is limited. In this case,  
710 the maximal emission capacity for VOC emission is restricted by the diffusive supply of VOC  
711 and is not influenced by the ACR. In this scenario, diffusion of the VOC within the solid  
712 material is the phenomenon limiting emission from the material studied. (ii) For all VOCs  
713 monitored, including formaldehyde, diffusion within the solid material is the phenomenon  
714 limiting emissions. The enhanced formaldehyde emission rate when the ACR increases  
715 could be explained by hydrolysis of binding resin leading to the release of formaldehyde (He

716 et al., 2019). This hydrolysis may be promoted by the water present in the fresh air entering  
 717 the chamber. Formaldehyde formation as a result of resin hydrolysis would continuously  
 718 supply formaldehyde for emission ( $C_0$ ), especially at the material's surface. (iii) A  
 719 combination of the two previous hypotheses – formaldehyde diffusion within the material is  
 720 high supplying the material's surface, and the PB resin is continuously hydrolysed to  
 721 generate formaldehyde – could explain the enhanced formaldehyde emission rate in the high  
 722 ACR conditions.

723 Although the analytical equation was solved for an airtight chamber, the convective mass  
 724 transfer coefficient through the boundary layer  $h_i$  appears in the equation, since the mixing  
 725 fan induced a convective airflow inside the chamber. However, some difficulties in the  
 726 determination of  $D_i$  were encountered due to an unrealistic convective mass transfer  
 727 coefficient. This parameter did not provide a satisfactory correlation between the  
 728 experimental curve and the solution to the analytical equation. Axley (1991) indicates that the  
 729 convective mass transfer coefficient  $h_i$  can be calculated using theoretical equations based  
 730 on ideal cases. These equations mainly depend on two unreliable parameters: the mean fluid  
 731 velocity near to the material's surface ( $U$ ) and the length of the surface in the direction of the  
 732 flow ( $L$ ).  $U$  and  $L$  can vary considerably from one case to another. Therefore, the convective  
 733 mass transfer coefficients must be calculated once again using  $U$  and  $L$  values that agree  
 734 better with all the VOCs studied from Equation 3. In this paper,  $h_i$  only depended on the  
 735 molecular diffusivity of the VOCs in air. All convective mass transfer coefficients are reported  
 736 in Table 6.

737 **Table 6: Convective mass transfer coefficients  $h_i$  for the eight VOCs emitted from the selected**  
 738 **PB ( $m.s^{-1}$ ).**

i	Formaldehyde	Acetone	Acetaldehyde	Propanal	Butanal	Pentanal	Hexanal	Terpenes
$h_i$ ( $m.s^{-1}$ )	$1.61 \times 10^{-4}$	$1.26 \times 10^{-4}$	$1.26 \times 10^{-4}$	$1.12 \times 10^{-4}$	$1.01 \times 10^{-4}$	$9.41 \times 10^{-5}$	$8.84 \times 10^{-5}$	$7.66 \times 10^{-5}$

739 According to several publications (Zhang and Niu, 2004, 2003; Zhang et al., 2018, 2003),  
 740 convective mass transfer usually varies from  $1.0 \times 10^{-4}$  to  $1.0 \times 10^{-2}$   $m.s^{-1}$  for building materials.  
 741 Compared to published  $h_i$  values, the VOCs emitted from our PB present low convective

742 mass transfer coefficients (Table 6). Since convective mass transfer through the boundary  
743 layer is affected by the airflow over the material surface, especially its velocity, the low  $h_i$   
744 values could explain the negligible impact of the air velocity over the material's surface on  
745 VOC emissions reported above. These low convective mass transfer coefficients corroborate  
746 the hypothesis that VOC emissions from the PB studied here are mainly controlled by their  
747 diffusion within the material.

748 If Equation 3 is reworked to a different form using Equation 5, the positive correlation  
749 between the convective mass transfer coefficients  $h_i$  and the molecular diffusion in air  $\delta_i$  can  
750 be highlighted. Since molecular diffusion in air is negatively correlated with molar weight  
751 according to Equation 6, it results in negative correlation relationship between the coefficient  
752  $h_i$  and molar weight. Thus, it can be observed that the convective mass transfer coefficient  $h_i$   
753 is negatively correlated with the molar weight of VOCs. Among the VOCs monitored,  
754 formaldehyde had the lowest molar weight, at  $30.03 \text{ g}\cdot\text{mol}^{-1}$  and the highest convective mass  
755 transfer coefficient. Conversely, terpenes had the lowest convective mass transfer coefficient  
756 and the highest molar weight ( $136.24 \text{ g}\cdot\text{mol}^{-1}$ ).

#### 757 **4. Conclusion**

758 With a view to reducing VOC concentrations in indoor environments, ventilation is known to  
759 have a significant effect on VOC emissions. However, ventilation could differentially affect  
760 the behaviour of individual VOCs emitted from a single solid material. To understand the  
761 physical phenomenon of VOC emission, in this study, the individual behaviours of VOCs  
762 were assessed using two distinct scales of study. Firstly, the respective impacts of air  
763 velocity and the ACR on VOC emissions were measured. This overall assessment of the  
764 influence of ventilation highlighted the non-conformist behaviour of formaldehyde with  
765 respect to the ACR even through changes to the speed of the air flowing over the material's  
766 surface did not significantly alter the emission rates for any of the VOCs studied. By  
767 determining the key emission parameters ( $K_i$ ,  $C_{0,i}$ ,  $D_i$ ) for the VOCs studied, we discovered  
768 that formaldehyde had higher partitioning and diffusion coefficients than the other

769 compounds. These significant differences in diffusion and partitioning coefficients between  
770 formaldehyde and other VOCs allowed us to propose physical interpretations of the data  
771 related to the specific influence of the ACR on the formaldehyde emission rate. VOC  
772 emissions are mainly controlled by the VOC's diffusion within the material, which is the  
773 limiting process in VOC emission for our solid material. When the ACR increased, the  
774 formaldehyde emission rate was enhanced due to its higher diffusion and partitioning  
775 coefficients compared to other VOCs. A detailed sensitivity analysis of the experimental  
776 method should be carried out to assess the quality of the data obtained. This analysis would  
777 be worth a full paper.

778 The influence of environmental parameters on VOC emissions will need to be further  
779 investigated as temperature has been observed to have a significant effect on overall VOC  
780 emissions at chamber scale. The influence of the environmental conditions (temperature and  
781 RH) on key emission parameters ( $K_i$ ,  $C_{0,i}$ ,  $D_i$ ) should then be assessed at material scale.  
782 Since the impact of environmental parameters on emission parameters has not been  
783 extensively documented, with data only available for formaldehyde, relationships between  
784 environmental parameters and each emission parameters could be proposed for several  
785 VOCs emitted from a single solid material.

786 This paper provides new insight into the mechanisms governing VOC emissions. Moreover,  
787 some VOCs were shown to display unique behaviour with respect to ventilation, in particular  
788 formaldehyde. This observation underlines the need to individually consider the VOCs  
789 monitored when investigating their emission rates from solid materials in indoor  
790 environments. Finally, the enhanced formaldehyde emission rate as a function of the ACR  
791 calls for care to be taken and for the singular behaviour of formaldehyde to be considered  
792 when establishing indoor air quality prevention strategies based on ventilation.

### 793 **Acknowledgements**

794 This work was achieved in the frame of ESQUISSE project, funded by INRS. It results from a  
795 collaboration between INRS and IMT Lille Douai. Florent Caron acknowledges INRS for  
796 funding his PhD.

## 797 **References**

798 Axley, J.W., 1991. Adsorption Modelling for Building Contaminant Dispersal Analysis. *Indoor*  
799 *Air* 1, 147–171. <https://doi.org/10.1111/j.1600-0668.1991.04-12.x>

800 Bodalal, A., Zhang, J.S., Plett, E.G., 2000. A method for measuring internal diffusion and  
801 equilibrium partition coefficients of volatile organic compounds for building materials.  
802 *Building and Environment* 10.

803 Colombo, A., De Bortoli, M., Knoppel, H., Pecchio, E., Vissers, H., 1993. Adsorption Of  
804 Selected Volatile Organic Compounds On A Carpet, A Wall Coating, And A Gypsum  
805 Board In A Test Chamber. *Indoor Air* 3, 276–282. <https://doi.org/10.1111/j.1600-0668.1993.00009.x>

807 Cox, S.S., Liu, Z., Little, J.C., Howard-Reed, C., Nabinger, S.J., Persily, A., 2010.  
808 Diffusion-controlled reference material for VOC emissions testing: proof of concept.  
809 *Indoor Air* 20, 424–433. <https://doi.org/10.1111/j.1600-0668.2010.00666.x>

810 de Gennaro, G., de Gennaro, L., Mazzone, A., Porcelli, F., Tutino, M., 2014. Indoor air  
811 quality in hair salons: Screening of volatile organic compounds and indicators based  
812 on health risk assessment. *Atmospheric Environment* 83, 119–126.  
813 <https://doi.org/10.1016/j.atmosenv.2013.10.056>

814 Dorieh, A., Mahmoodi, N.O., Mamaghani, M., Pizzi, A., Mohammadi Zeydi, M., moslemi, A.,  
815 2019. New insight into the use of latent catalysts for the synthesis of urea  
816 formaldehyde adhesives and the mechanical properties of medium density  
817 fiberboards bonded with them. *European Polymer Journal* 112, 195–205.  
818 <https://doi.org/10.1016/j.eurpolymj.2019.01.002>

819 Dunky, M., 1998. Urea–formaldehyde (UF) adhesive resins for wood. *International Journal of*  
820 *Adhesion and Adhesives* 18, 95–107. [https://doi.org/10.1016/S0143-7496\(97\)00054-](https://doi.org/10.1016/S0143-7496(97)00054-)

821 7

822 Fuller, E.N., Ensley, K., Giddings, J.C., 1969. Diffusion of halogenated hydrocarbons in  
823 helium. The effect of structure on collision cross sections. *The Journal of Physical*  
824 *Chemistry* 73, 3679–3685. <https://doi.org/10.1021/j100845a020>

825 Fuller, E.N., Giddings, J.C., 1965. A Comparison of Methods for Predicting Gaseous  
826 Diffusion Coefficients. *Journal of Chromatographic Science* 3, 222–227.  
827 <https://doi.org/10.1093/chromsci/3.7.222>

828 Fuller, E.N., Schettler, P.D., Giddings, J. Calvin., 1966. NEW METHOD FOR PREDICTION  
829 OF BINARY GAS-PHASE DIFFUSION COEFFICIENTS. *Industrial & Engineering*  
830 *Chemistry* 58, 18–27. <https://doi.org/10.1021/ie50677a007>

831 Harb, P., Locoge, N., Thevenet, F., 2018. Emissions and treatment of VOCs emitted from  
832 wood-based construction materials: Impact on indoor air quality. *Chemical*  
833 *Engineering Journal* 354, 641–652. <https://doi.org/10.1016/j.cej.2018.08.085>

834 He, Z., Xiong, J., Kumagai, K., Chen, W., 2019. An improved mechanism-based model for  
835 predicting the long-term formaldehyde emissions from composite wood products with  
836 exposed edges and seams. *Environment International* 132, 105086.  
837 <https://doi.org/10.1016/j.envint.2019.105086>

838 Huang, L., Mo, J., Sundell, J., Fan, Z., Zhang, Y., 2013. Health Risk Assessment of  
839 Inhalation Exposure to Formaldehyde and Benzene in Newly Remodeled Buildings,  
840 Beijing. *PLOS ONE* 8, e79553. <https://doi.org/10.1371/journal.pone.0079553>

841 Huang, S., Wei, W., Weschler, L.B., Salthammer, T., Kan, H., Bu, Z., Zhang, Y., 2017. Indoor  
842 formaldehyde concentrations in urban China: Preliminary study of some important  
843 influencing factors. *Science of The Total Environment* 590–591, 394–405.  
844 <https://doi.org/10.1016/j.scitotenv.2017.02.187>

845 Huang, S., Xiong, J., Zhang, Y., 2013. A rapid and accurate method, ventilated chamber C-  
846 history method, of measuring the emission characteristic parameters of  
847 formaldehyde/VOCs in building materials. *Journal of Hazardous Materials* 261, 542–  
848 549. <https://doi.org/10.1016/j.jhazmat.2013.08.001>

849 Huangfu, Y., Lima, N.M., O’Keeffe, P.T., Kirk, W.M., Lamb, B.K., Pressley, S.N., Lin, B.,  
850 Cook, D.J., Walden, V.P., Jobson, B.T., 2019. Diel variation of formaldehyde levels  
851 and other VOCs in homes driven by temperature dependent infiltration and emission  
852 rates. *Building and Environment* 159, 106153.  
853 <https://doi.org/10.1016/j.buildenv.2019.05.031>

854 Hult, E.L., Willem, H., Price, P.N., Hotchi, T., Russell, M.L., Singer, B.C., 2015.  
855 Formaldehyde and acetaldehyde exposure mitigation in US residences: in-home  
856 measurements of ventilation control and source control. *Indoor Air* 25, 523–535.  
857 <https://doi.org/10.1111/ina.12160>

858 Hun, D.E., Corsi, R.L., Morandi, M.T., Siegel, J.A., 2010. Formaldehyde in Residences:  
859 Long-Term Indoor Concentrations and Influencing Factors. *Indoor Air*.  
860 <https://doi.org/10.1111/j.0905-6947.2010.00644.x>

861 Kelly, T.J., Smith, D.L., Satola, J., 1999. Emission Rates of Formaldehyde from Materials  
862 and Consumer Products Found in California Homes 8.

863 Knudsen, H.N., Kjaer, U.D., Nielsen, P.A., Wolkoff, P., 1999. Sensory and chemical  
864 characterization of VOC emissions from building products: impact of concentration  
865 and air velocity. *Atmospheric Environment* 33, 1217–1230.  
866 [https://doi.org/10.1016/S1352-2310\(98\)00278-7](https://doi.org/10.1016/S1352-2310(98)00278-7)

867 Liu, Z., Howard-Reed, C., Cox, S.S., Ye, W., Little, J.C., 2014. Diffusion-controlled reference  
868 material for VOC emissions testing: effect of temperature and humidity. *Indoor Air* 24,  
869 283–291. <https://doi.org/10.1111/ina.12076>

870 Liu, Z., Ye, W., Little, J.C., 2013. Predicting emissions of volatile and semivolatile organic  
871 compounds from building materials: A review. *Building and Environment* 64, 7–25.  
872 <https://doi.org/10.1016/j.buildenv.2013.02.012>

873 Myers, G.E., 1982. Formaldehyde dynamic air contamination by hardwood plywood: effects  
874 of several variables and board treatments. *Forest products journal* 32, 20–25.

875 Nirlo, E.L., Crain, N., Corsi, R.L., Siegel, J.A., 2014. Volatile organic compounds in fourteen  
876 U.S. retail stores. *Indoor Air* 24, 484–494. <https://doi.org/10.1111/ina.12101>

877 Offermann, F.J., Hodgson, A.T., 2011. Emission Rates of Volatile Organic Compounds in  
878 New Homes 7.

879 Risholm-Sundman, M., 1999. Determination of Formaldehyde Emission with Field and  
880 Laboratory Emission Cell (FLEC) - Recovery and Correlation to the Chamber Method.  
881 Indoor Air 9, 268–272. <https://doi.org/10.1111/j.1600-0668.1999.00006.x>

882 Robert, L., Guichard, R., Klingler, J., Cochet, V., 2018. IMPACT OF VENTILATION ON  
883 INDOOR AIR QUALITY IN A SPORTS STORE 7.

884 Salthammer, T., Mentese, S., Marutzky, R., 2010. Formaldehyde in the Indoor Environment.  
885 Chemical Reviews 110, 2536–2572. <https://doi.org/10.1021/cr800399g>

886 Shang, Y., Li, B., Baldwin, A.N., Ding, Y., Yu, W., Cheng, L., 2016. Investigation of indoor air  
887 quality in shopping malls during summer in Western China using subjective survey  
888 and field measurement. Building and Environment 108, 1–11.  
889 <https://doi.org/10.1016/j.buildenv.2016.08.012>

890 Smith, J.F., Gao, Z., Zhang, J.S., Guo, B., 2009. A New Experimental Method for the  
891 Determination of Emittable Initial VOC Concentrations in Building Materials and  
892 Sorption Isotherms for IVOCs. CLEAN – Soil, Air, Water 37, 454–458.  
893 <https://doi.org/10.1002/clen.200900003>

894 Tiffonnet, A.-L., 2000. Contribution à l'analyse de la Qualité de l'Air Intérieur: Influence des  
895 transports de Composés Organiques Volatils (COV) entre les parois et l'ambiance  
896 (PhD Thesis). La Rochelle.

897 Tiffonnet, A.-L., Marion, M., Makhoulfi, R., Blondeau, P., 2006. Etude des résistances au  
898 transfert de COV entre une paroi et l'ambiance 9.

899 Uhde, E., Borgschulte, A., Salthammer, T., 1998. Characterization of the field and laboratory  
900 emission cell—FLEC: Flow field and air velocities. Atmospheric Environment 32, 773–  
901 781. [https://doi.org/10.1016/S1352-2310\(97\)00345-2](https://doi.org/10.1016/S1352-2310(97)00345-2)

902 Wolkoff, P., 1998. Impact of air velocity, temperature, humidity, and air on long-term voc  
903 emissions from building products. Atmospheric Environment 32, 2659–2668.  
904 [https://doi.org/10.1016/S1352-2310\(97\)00402-0](https://doi.org/10.1016/S1352-2310(97)00402-0)

905 Wolkoff, P., Nielsen, G.D., 2001. Organic compounds in indoor air—their relevance for  
906 perceived indoor air quality? *Atmospheric Environment* 35, 4407–4417.

907 Xiong, J., Zhang, Y., Huang, S., 2011. Characterisation of VOC and Formaldehyde Emission  
908 from Building Materials in a Static Environmental Chamber: Model Development and  
909 Application: Indoor and Built Environment.  
910 <https://doi.org/10.1177/1420326X103874801>

911 Xiong, J., Zhang, Y., Wang, X., Chang, D., 2008. Macro–meso two-scale model for predicting  
912 the VOC diffusion coefficients and emission characteristics of porous building  
913 materials. *Atmospheric Environment* 42, 5278–5290.  
914 <https://doi.org/10.1016/j.atmosenv.2008.02.062>

915 Xu, J., Zhang, J.S., 2011. An experimental study of relative humidity effect on VOCs'  
916 effective diffusion coefficient and partition coefficient in a porous medium. *Building  
917 and Environment* 46, 1785–1796. <https://doi.org/10.1016/j.buildenv.2011.02.007>

918 Yoon, H.I., Hong, Y.-C., Cho, S.-H., Kim, H., Kim, Y.H., Sohn, J.R., Kwon, M., Park, S.-H.,  
919 Cho, M.-H., Cheong, H.-K., 2010. Exposure to volatile organic compounds and loss of  
920 pulmonary function in the elderly. *European Respiratory Journal* 36, 1270–1276.  
921 <https://doi.org/10.1183/09031936.00153509>

922 Zhang, L.Z., Niu, J.L., 2004. Modeling VOCs emissions in a room with a single-zone multi-  
923 component multi-layer technique. *Building and Environment* 39, 523–531.  
924 <https://doi.org/10.1016/j.buildenv.2003.10.005>

925 Zhang, L.Z., Niu, J.L., 2003. Laminar fluid flow and mass transfer in a standard field and  
926 laboratory emission cell. *International Journal of Heat and Mass Transfer* 10.

927 Zhang, X., Cao, J., Wei, J., Zhang, Y., 2018. Improved C-history method for rapidly and  
928 accurately measuring the characteristic parameters of formaldehyde/VOCs emitted  
929 from building materials. *Building and Environment* 143, 570–578.  
930 <https://doi.org/10.1016/j.buildenv.2018.07.030>

931 Zhang, Y., Deng, Q., Qian, H., Mo, J., 2012. Research advance report of indoor environment  
932 and health in China. China Architecture & Building PressChina.

933 Zhang, Y., Yang, R., Zhao, R., 2003. A model for analyzing the performance of photocatalytic  
934 air cleaner in removing volatile organic compounds. *Atmospheric Environment* 37,  
935 3395–3399. [https://doi.org/10.1016/S1352-2310\(03\)00357-1](https://doi.org/10.1016/S1352-2310(03)00357-1)

936 Zhou, X., Liu, Y., Liu, J., 2018. Alternately airtight/ventilated emission method: A universal  
937 experimental method for determining the VOC emission characteristic parameters of  
938 building materials. *Building and Environment* 130, 179–189.  
939 <https://doi.org/10.1016/j.buildenv.2017.12.025>